Optimal Detection of Acute Lymphoblastic Leukemia Using Deep Transfer Learning Model

Rana Adinda Manalus Fata, Indrarini Dyah Irawati*[ID], Sugondo Hadiyoso[ID]

School of Applied Science, Telkom University, Bandung 40287, Indonesia

Corresponding Author Email: indrarini@telkomuniversity.ac.id

ABSTRACT

Acute Lymphoblastic Leukemia (ALL), a rapidly progressing malignancy originating from hematopoietic cells, necessitates prompt and precise diagnosis due to its potential lethality within a short span of months. Technological advancements are therefore pivotal in aiding medical practitioners to reduce the probability of human error, expedite diagnosis and subsequently, improve patient outcomes. This study presents a novel system leveraging Convolutional Neural Networks (CNNs), capable of diagnosing ALL through image analysis of affected cells. Our proposed system employs two well-established CNN architectures, VGG16 and ResNet50, coupled with two optimization algorithms, Adam and RMSprop, to classify image data into two distinct categories. The utilized dataset, C-NMC Leukemia 2019, was subjected to a variety of test scenarios involving differing epoch variations (10, 20, 30, 40, 50, 60, 80, and 100) and a consistent learning rate of 0.0001. The results suggest that the proposed system exhibits superior performance when utilizing the VGG16 architecture in conjunction with the Adam optimizer, achieving a training accuracy of 93.80% and a testing accuracy of 87.00%. The findings of this study accentuate the potential of integrating deep learning techniques into the diagnostic process of ALL, thereby facilitating rapid, precise detection and ultimately contributing to the improvement of patient prognosis.

1. INTRODUCTION

Acute Lymphoblastic Leukemia (ALL) represents a prevalent malignancy of white blood cells among children, with the peak incidence noted in the age group of 1-4 years, accounting for approximately 80% of pediatric cases [1]. The rapid progression of this disease underscores the essential need for swift and accurate diagnostic procedures, given its potential fatality within a few months if left untreated [1]. Hence, advancements in technology are being actively pursued in the medical field, with the objective of reducing human errors in diagnosis and facilitating accurate and timely disease detection [2, 3].

The advent of digital image processing techniques has significantly transformed various sectors, notably in healthcare [4, 5]. These techniques have been particularly useful in early-stage detection and classification of diseases or cancers via blood cell image analysis, as reported in several studies [6-12]. In one such study, the authors employed color-based k-means technique for lymphocyte extraction from segmented images for the detection and classification of ALL [7]. The use of combined techniques, including the Gray-Level Co-occurrence Matrix (GLCM) and Gray-Level Run-Length Matrix (GLRLM) for nuclear feature extraction, Principal Component Analysis (PCA) for image resizing, and Support Vector Machine (SVM) for classification, resulted in an accuracy of 96.00% and sensitivity of 92.64% [7].

Deep Learning, a subset of machine learning, has shown immense potential in processing large data volumes. Among the various deep learning techniques, Convolutional Neural Networks (CNNs) have emerged as a powerful tool for image recognition and processing. Inspired by the image recognition systems present in the visual cortex of human and animal brains, CNNs are specifically designed to process image data [13]. The potential of CNNs in the early detection and classification of diseases like ALL, therefore, warrants further investigation to enhance patient outcomes.

In the study [8], this study explores the performance of the CNN, MobilenetV2 and ResNet18 architectures for datasets from ALLIDB1 and ALLIDB2. The results of 70% training and 30% testing show that the accuracy level of each dataset is 99.39% and 97.18%. In another study [9], the CNN transfer learning technique was used to improve accuracy in detecting ALL in a histopathology database with a limited number of samples. CNN classified tissue types from the histopathological database and then performed refinements to the ALL database to detect the presence of lymphoblasts considering a multi-label data set of a much larger number of samples and classes than the existing literature. Another study extracts features from White Blood Cell (WBC) images using the VGG Net architecture, which has been trained on Image Net combined with feature extraction using the Salp Swarm Algorithm (SESSA). This method can outperform other convolution methods with an accuracy of 96.11% in Dataset 1 and 87.90% in Dataset 2 [10].

Based on previous research studies, there are still many opportunities to explore classification techniques in ALL datasets using DNN. Therefore, this study aims to optimize ALL classification by comparing the VGG16 and ResNet50 architectures with improved performance using the Adam and RMSprop optimizers on various datasets. The classification results are divided into two classes: the normal cell class and

the cancer cell class (ALL). System performance is measured based on accuracy, precision, f1-score, and recall parameters.

2. MATERIAL AND METHODS

2.1 Cancer cell datasets

Leukemia is a disorder of human blood cells in which the production of leukocytes is abnormal. Based on the proliferation rate, these disorders can be classified as acute or chronic, while based on the originating cells are classified as myeloid or lymphoid. The predominant subtypes are acute myeloid leukemia (AML) and chronic myeloid leukemia (CML), which involve the myeloid chains and ALL, and chronic lymphocytic leukemia (CLL), involving the lymphoid chain. This study determined the classification for ALL that affects 80% of pediatrics. Proper treatment can improve survival rates [14].

The dataset used in this study was taken from the ALL Challenge dataset of ISBI 2019 (C-NMC 2019) collected by The Cancer Imaging Archive (TCIA) Public Access. The image is saved in .bmp or bitmap format with 10,661 consisting of 7,272 cancer and 3,389 normal. An example of a microscopic image of Leukemia is shown in Figure 1.

(a) (b)
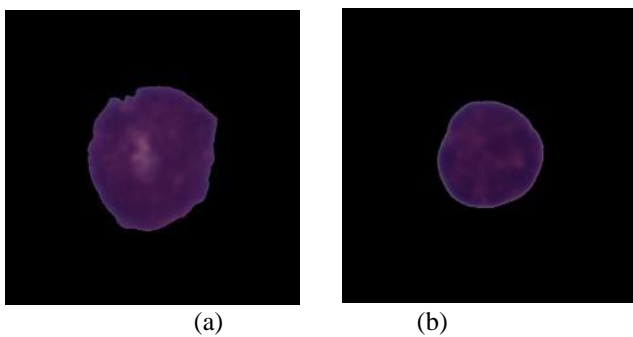
Figure 1. Leukemia (a) Normal blood (b)

2.2 Convolutional neural network
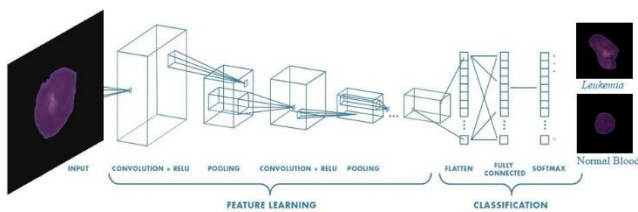
Figure 2. Basic arsitektur CNN

CNN is included in the category of deep learning because of the depth of the network. CNN is the most popular neural network method and is of great interest to many researchers in the pattern recognition of an object. CNN is capable of handling high-dimensional data such as video and images. The way CNN works is similar to neural networks in general. The only difference is that it uses a 2-dimensional or high-dimensional kernel for each unit in the CNN layer to be convoluted. The kernel in CNN is used to combine spatial features with a spatial form that resembles the input medium. Then CNN uses various parameters to reduce the number to make learning easier [15]. The output of the convolutional layer is called a feature map describing the image's unique

characteristics. The convolutional layer consists of a filter that performs the convolution process on the input image matrix. The CNN architecture consists of several layers: the convolution layer, activation layer function, pooling layer, and fully connected layer. The CNN illustration in this study can be seen in Figure 2.

2.3 VGG16 architecture

The VGG16 architecture is a CNN model first proposed by Simonyan and Zisserman [16]. The model was successful at 92.7% and is the top 5 test accuracy on the ImageNet dataset, which consists of 14 million images from 10,000 different classes. Figure 3 shows the basic architecture of VGG16 used in this study.
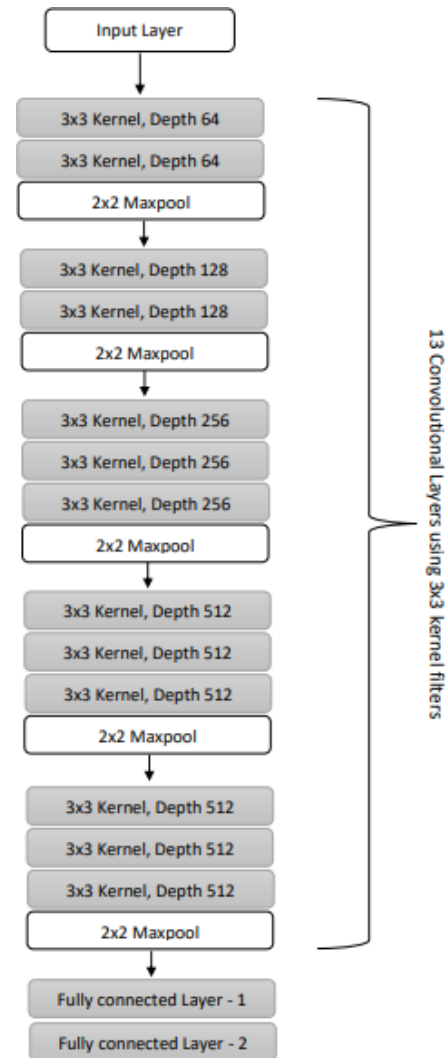
Figure 3. VGG16 architecture

2.4 ResNet50 architecture

A proposed shortcut connection in the CNN architecture aims to speed up the process while increasing the accuracy of the residual network. The shortcut connection concept is known as the ResNet architecture which is related to the vanishing gradient problem that arises when attempting to deepen the network structure. The deeper a network can lead to a vanishing gradient problem that can make the gradient very small which results in decreased performance or accuracy [17]. In this study, ResNet50 was used as shown in Figure 4.

2.5 Optimizers

The selection of the optimizer is the main step in the deep learning channel. The optimization algorithm aims to find the optimal weight, minimize errors and maximize accuracy. During training, the parameters or weights of the model are changed to try and minimize the loss function to predict as accurately as possible. This optimization is done by adding several hyperparameters to the designed CNN architecture [18]. In this study, a comparison was made between the RMSprop optimizer and Adam.
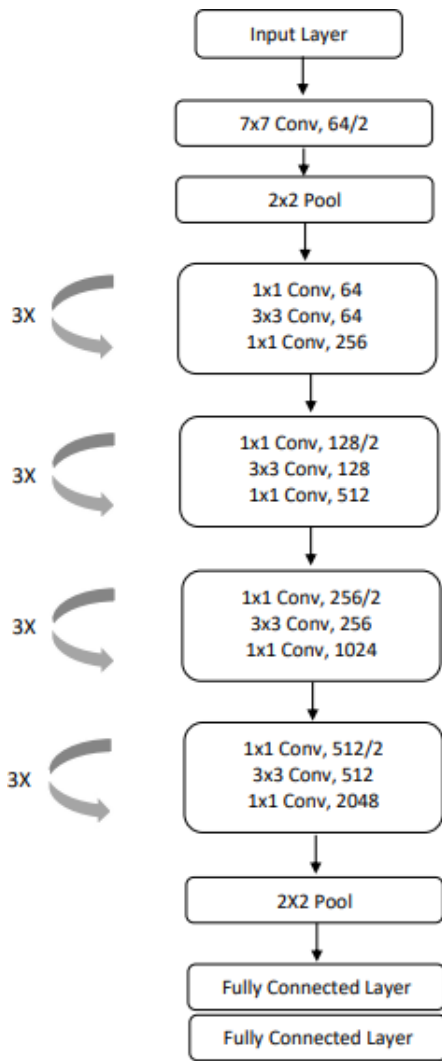
Figure 4. ResNet50 architecture

RMSprop is an optimizer that utilizes the latest gradient magnitude to normalize the gradient, which keeps the moving average above the root mean square gradient; hence it is called RMS [19]. Adam is an optimization algorithm that can be used instead of the classic stochastic gradient descent procedure to update the network weights based on the training data iteratively. Adam is a popular deep-learning algorithm because it quickly achieves good results [20].

2.6 System model

Figure 5 shows a flow chart of our proposed approach for ALL detection. All labelled images are uploaded to the database in the dataset input stage. After pre-processing, 80% or 8,528 of the training data were taken from the total dataset

and 20% or 2,133 for the test data. This CNN model uses transfer learning with pre-trained models from VGG16 and ResNet50 and can then be forwarded to the dense layer (512) and ReLU activation. Also, for the output layer, use dense (2) and the softmax activation function. The design of the CNN model used is shown in Figure 6.

The training was carried out using epochs 10, 20, 30, 40, 50, 60, 80, and 100 and a learning rate of 0.0001. The batch size used is 32 by adding the optimizer Adam and RMSprop to achieve the optimal value and, in addition, using an additional hyperparameter with a decay step of 900 and a decay rate of 0.95 and using a binary cross-entropy loss function.

In the testing phase, the test is carried out on 20% of the total dataset. Performance testing is done by calculating the confusion matrix. Model evaluation is done by monitoring the number of True Positive (TP), True Negative (TN), False Positive (FP), and False Negative (FN). From these data, accuracy, precision, recall and f1-score can be calculated from the resulting model. From these values, accuracy, precision, recall, and f1-score can be calculated as expressed by Eqns. (1), (2), (3) and (4) below [21].
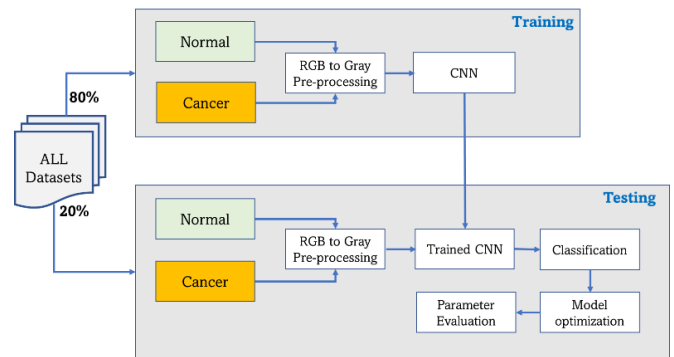
Figure 5. Flowchart of the ALL detection process
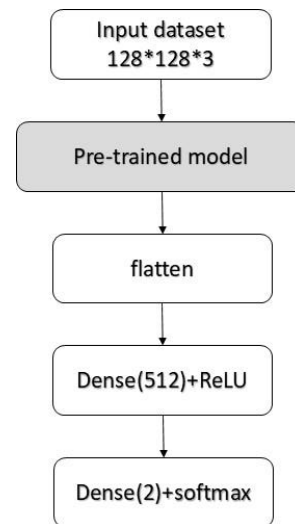
Figure 6. Proposed CNN architectural model

$$accuracy = \frac{TP + TN}{TP + TN + FP + FN} \qquad (1)$$

$$precision = \frac{TP}{TP + FP} \qquad (2)$$

$$recall = \frac{TP}{TP + FN} \qquad (3)$$

$$F1score = \frac{2 * recall * precision}{recall + precision} \qquad (4)$$

In the test, two scenarios were used: scenario A for the VGG16 architecture and scenario B for the ResNet50 architecture. In both scenarios, training was conducted using an architectural model with a transfer learning system. This process uses different optimizers, namely Adam and RMSprop, as well as epochs 10, 20, 30, 40, 50, 60, 80 and 100, with a learning rate of 0.0001.

3. RESULTS AND DISCUSSION

3.1 Model training results

The results of the training model for scenario A are presented in Table 1. This scenario shows that the best training accuracy is 93.80% with 100 epochs and using the Adam optimizer. Meanwhile, the lower accuracy is 84.36% with an epoch value of 10 and the optimizer prop. Scenario A is superior when using the Adam optimizer compared to prop. The variation of epochs during training is quite influential, where the greater the number of epochs, the accuracy obtained will also be higher. However, not for models that use the RMSprop optimizer, at epoch 40, the accuracy decreases to 86.83%. Table 2 shows the training resuls of scenario B. The best accuracy was obtained at epoch 100 on both optimizers. In Adam, the accuracy is 81.63%, while in RMSprop is 81.70%. The accuracy results in scenario A using VGG16 are higher than in scenario B using ResNet50.

In contrast to scenario A, scenario B has a smaller training accuracy than scenario A for all epochs and optimizers. In this model, the accuracy is obtained with a range of 80-81%, and the highest accuracy is 81.81%. These results were obtained at epoch 80 with the RMSprop optimizer. In scenario B, accuracy regularly increases when using the RMSprop optimizer compared to the Adam optimizer.

Table 1. Scenario A training results

Epoch	Adam	RMSprop
10	84.73%	84.36%
20	87.85%	86.49%
30	89.74%	87.72%
40	89.45%	86.83%
50	91.50%	89.83%
60	91.97%	89.69%
80	92.33%	91.65%
100	93.80%	92.75%

Table 2. Scenario B training results

Epoch	Adam	RMSprop
10	80.08%	80.18%
20	80.87%	80.96%
30	81.07%	80.98%
40	80.97%	80.82%
50	81.14%	81.23%
60	81.19 %	81.07%
80	81.60%	81.81%
100	81.63%	81.70%

The training curve for scenario A for each epoch and optimizer is presented in Figure 7. Meanwhile, the training curve for scenario B is shown in Figure 8. This curve will make it easier to observe in detail the effect of epochs on the resulting accuracy.
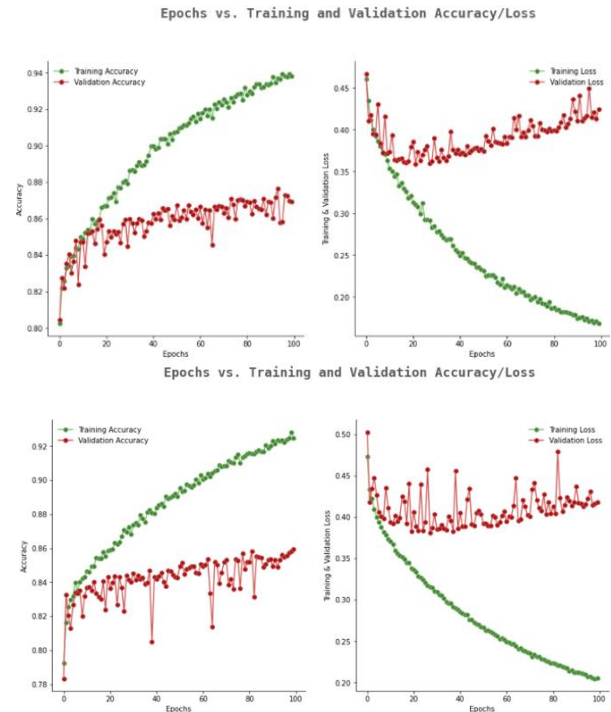
Figure 7. Scenario A training curve with Adam and RMSprop (epoch 10 - epoch 100)
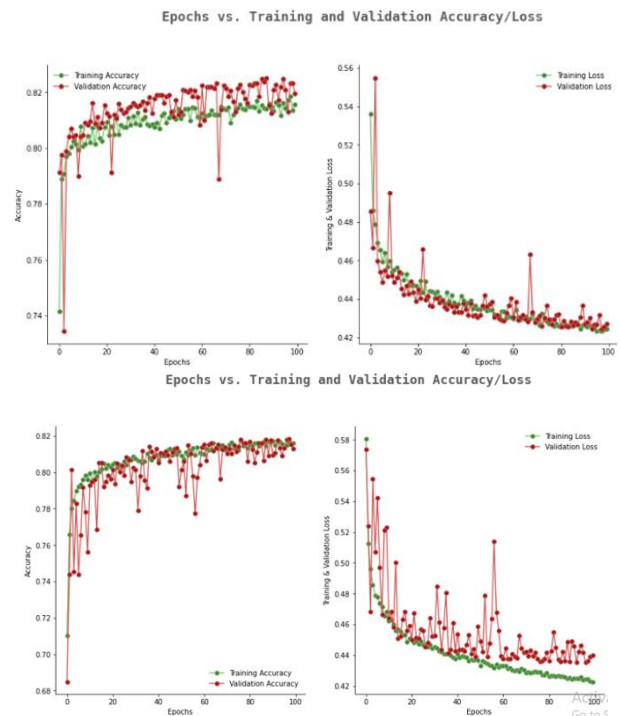
Figure 8. Scenario B training curve with Adam optimizer and RMSprop (epoch 10 - epoch 100)

The training curves presented in Figure 7 and Figure 8 show that the Adam optimizer is faster at learning than RMSprop. Even though learning has high-performance results, the curve shows that the gap between training and validation is quite far compared to scenario B. Figure 7 also shows that validation accuracy can be more optimal. Loss validation accuracy has yet to reach a minimum value. In general, processes

experience a more stable decrease in accuracy. Whereas scenario B shows that the learning process is more stable with scenario A, and the gap between accuracy training and validation is small-the disadvantage, enough to reach the minimum value.

3.2 Test model result

Figure 9 shows a graph of the accuracy of the testing phase. This simulation shows that all model tests carried out in scenario A get superior results compared to scenario B. At the best performance, it is known that the application of the VGG16 transfer learning model in large dataset cases gets the highest accuracy results compared to the ResNet50 model. Test scenario A using the VGG16 model has an accuracy test result of around 84-87%. When using ten epochs, it has the same accuracy as the two optimizers, which is 84%; when using 20 epochs, the RMSprop optimizer has 86% accuracy, while Adam's optimizer is 85%.

Furthermore, RMSprop optimizer often experiences ups and downs compared to Adam optimizer, which tends to be stable. These results are good for many data sets and the similarity of data sets when viewed visually. However, in scenario B, tested using the ResNet50 model, the test accuracy reached around 80-82%. The effect of epoch variation in scenario B is quite stable and does not decrease the accuracy of results. Here it can be seen that if the number of epochs increases, the accuracy of results will increase. The difference between the two scenarios is small, but in scenario A, pre-trained VGG16 is more suitable for large dataset research cases than ResNet50.
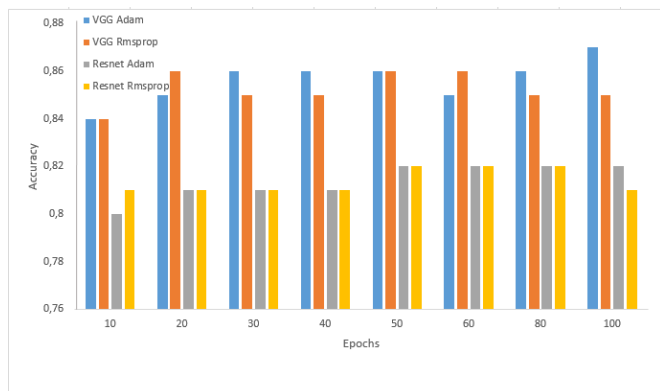
Figure 9. Results of the test model

Table 3. Recall, precision and f1-score with VGG16 and Adam's Optimize

Epoch	Recall	Prec.	F1-Score
10	0.76	0.86	0.79
20	0.81	0.84	0.82
30	0.82	0.85	0.82
40	0.79	0.86	0.82
50	0.82	0.84	0.83
60	0.81	0.83	0.82
80	0.81	0.87	0.83
100	0.81	0.87	0.84
Totals	0.81	0.85	0.82

Tables 3 and 4 show the average recall value, precision and f1-score. It can be seen that the highest overall recall value was obtained when using the Adam optimizer with f1-score values

of 0.81 and 0.82, respectively. The precision value of the two optimizers is the same, 0.85.

Table 4. Recall, precision and f1-score with VGG16 and RMSprop's Optimizer

Epoch	Recall	Prec.	F1-Score
10	0.79	0.81	0.73
20	0.79	0.86	0.82
30	0.82	0.84	0.83
40	0.77	0.87	0.80
50	0.81	0.85	0.82
60	0.79	0.87	0.82
80	0.80	0.85	0.82
100	0.80	0.85	0.82
Totals	0.80	0.85	0.81

In the results of ResNet50, as shown in Tables 5 and 6, the Adam optimizer is still superior in recall and f1-score. The simulation results provide recall and f1-score of 0.76 and 0.77, respectively. As for the precision value, the difference in value is relatively very small. However, scenario B's simulation results show that the Adam optimizer's use produces the best performance.

Table 5. Recall, precision dan f1-score with ResNet50 and Optimizer Adam

Epoch	Recall	Prec.	F1-Score
10	0.77	0.77	0.77
20	0.75	0.80	0.76
30	0.75	0.80	0.79
40	0.76	0.79	0.77
50	0.76	0.79	0.77
60	0.76	0.79	0.77
80	0.76	0.81	0.78
100	0.75	0.81	0.77
Totals	0.76	0.80	0.77

Table 6. Recall, precision dan f1-score with ResNet50 and Optimizer RMSprop

Epoch	Recall	Prec.	F1-Score
10	0.72	0.81	0.74
20	0.75	0.79	0.77
30	0.74	0.80	0.76
40	0.77	0.79	0.78
50	0.76	0.80	0.77
60	0.75	0.80	0.77
80	0.75	0.80	0.77
100	0.73	0.81	0.75
Totals	0.75	0.80	0.76

Performance analysis of the proposed method is also carried out by comparing the model's performance with relevant previous studies. Table 7 compares the model's performance with similar leukemia datasets. The highest accuracy was obtained [9] with a value of 88.69%. However, it uses a smaller number of images. Meanwhile, in comparison with studies which used the CMNC leukemia dataset, the proposed method in this study outperformed studies [10, 21, 22]. In addition, for the same dataset as the author, namely research in the study [10], namely C-MNC_Leukemia 2019 with a total dataset of 10,661, an accuracy of 83.3% was obtained using the VGGNet (SESSA) model. Meanwhile, the authors get an accuracy value of 87.00% for the transfer learning system with VGG16. These results are superior to research [10, 22].

Table 7. Comparison with other studies

Study	Models	Dataset Names	Number of Images	Accuracy
[9]	TL-VGG16 TL-ResNet18	ALL-IDB2	260	88.69% 87.54%
[10]	VGGNet (SESSA)	CMNC Leukimia	10,661	83,30%
[22]	TL- ResNet101	CMNC Leukemia	1,867	85.11%
[23]	VGG16	CMNC Leukemia	10,661	80.01%
[24]	TL-VGG16	ALL-IDB2	260	82.46%
[25]	RAN-ResNet50	Malaria Cell	27,558	78.16%
Proposed	**TL-VGG16 TL-ResNet50**	**CMNC Leukemia**	**10.661**	**87.00% 82.00%**

4. CONCLUSION

In this study, a transfer learning model for the detection of leukemia has been simulated based on microscopic images of blood cells. Based on the results of the tests that have been carried out, it can be concluded that the CNN method using the VGG16 and ResNet50 architecture with a transfer learning system can detect white blood cell cancer or Acute Lymphoblastic Leukemia.

The best accuracy training results were obtained from all experiments on the VGG16 model architecture with Adam optimizers using 100 epochs, namely 93.80% and accuracy testing of 87.00%. In addition, the ResNet50 model also has accuracy training and accuracy testing values of 81.81% and 82.00%, respectively, using 80 epochs and RMSprop optimizers. The use of the Adam optimizers in the learning process is faster than the RMSprop optimizers. These results are good for many datasets and the similarities possessed by these datasets. Model performance evaluation can be measured through precision, recall, f1-score, and accuracy. The best performance is obtained by using Adam's optimizers. The results of this study are quite good because, in each scenario, the model with Adam's optimizers is superior.

REFERENCES

[1] America Cancer Society. (2014). About Acute Lymphocytic Leukemia (ALL). https://www.cancer.org/cancer/acute-lymphocytic-leukemia/about.html, accessed on Jun. 17, 2022.

[2] Esteva, A., Kuprel, B., Novoa, R.A., Ko, J., Swetter, S. M., Blau, H.M., Thrun. S. (2017). Dermatologist-level classification of skin cancer with deep neural network. Nature, 542(7639): 115-118. https://doi.org/10.1038/nature21056

[3] Kermany, D.S., Goldbaum, M., Cai, W., Valentim, C.C.S., Liang, H., Baxter, S.L., Mc Keown, A., Yang, G., Wu, X., Yan, F., Dong, J., Prasadha, M.K., Pei, J., Ting, M.Y.L., Zhu, J., Li, C., Hewett, S., Dong, J., Ziyar, I., Shi, A., Zhang, R., Zheng, L., Hou, R., Shi, W., Fu, X., Duan, Y., Huu, V.A.N., Wen, C., Zhang, E.D., Zhang, C.L., Li, O., Wang, X., Singer, M.A., Sun, X., Xu, J., Tafreshi, A., Lewis, M.A., Xia, H., Zhang, K. (2018). Identifying medical diagnoses and treatable diseases by image-based deep learning. Cell, 172(5): 1122-1131. https://doi.org/10.1016/j.cell.2018.02.010

[4] Irawati, I.D., Hadiyoso, S., Fahmi, A. (2021). Compressive sensing in lung cancer images for telemedicine application. The 4th International Conference on Electronics, Communications and ControlEngineering (ICECC), Seoul, South Korea, April, 2021, pp. 55-61. https://doi.org/10.1145/3462676.3462685

[5] Irawati, I.D., Larasaty, I.A., Hadiyoso, S. (2022). Comparisonof convolution neural network architecture for colon cancer classification. International Journal of Online and Biomedical Engineering, 18(3): 164-172. https://doi.org/10.3991/ijoe.v18i03.27777

[6] Hussein, N.J. (2021). Acute lymphoblastic leukemia classification with blood smear microscopic images using Taylor-MBO based SVM. Webology, 18: 357-366. https://doi.org/10.14704/WEB/V18SI02/WEB18104

[7] Das, P.K., Jadoun, P., Meher, S. (2020). Detection and classification of acute lymphocytic leukemia. IEEE-HYDCON, Hyderabad, India, 2020, pp. 1-5, https://doi.org/10.1109/HYDCON48903.2020.9242745

[8] Das, P.K., Meher, S. (2021). An efficient deep convolutional neural network based detection and classification of acute lymphoblastic leukemia. Expert System Application, 183: 115311. https://doi.org/10.1016/j.eswa.2021.115311

[9] Genovese, A., Hosseini, M.S., Piuri, V, Plataniotis, K.N., Scotti, F. (2021). Histopathological transfer learning for acute lymphoblastic leukemia detection. IEEE International Conference on Computational Intelligence and Virtual Environments for Measurement Systems and Applications (CIVEMSA), Hong Kong, China, pp. 1-6. https://doi.org/10.1109/CIVEMSA52099.2021.9493677

[10] Sahlol, A.T., Kollmannsberger, P., Ewees, A.A. (2020). Efficient classifcation of white blood cell leukemiawith improved swarm optimization of deep features. Scientific Reports, 10(2536): 2259-2261. https://doi.org/10.1038/s41598-020-59215-9

[11] Alzubaidi, L., Fadhel, M.A., Al-Shamma, O., Zhang, J., Duan, Y. (2020). Deep learning models for classification of red blood cells in microscopy images to aid in sickle cell anemia diagnosis. Electronics, 9(3): 427. https://doi.org/10.3390/electronics9030427

[12] Irawati, I.D., Hadiyoso, S., Budiman, G., Fahmi, A., Latip, R. (2022). A novel texture extraction-based compressive sensing for lung cancer classification. Journal of Medical Signals & Sensors, 12(4): 278-284. https://doi.org/10.4103/jmss.jmss_127_21

[13] Alzubaidi, L., Zhang, J., Humaidi, A.J., Al-Dujaili, A., Duan, Y., Al-Shamma, O., Santamaría, J., Fadhel, M.A., Al-Amidie, M., Farhan, L. (2021). Review of deep learning: Concepts, CNN architectures, challenges, applications, future directions. Journal of Big Data, 8(53): 1-74. https://doi.org/10.1186/s40537-021-00444-8

[14] Chennamadhavuni, A., Lyengar, V., Mukkamalla, S. K. R., Shimanovsky, A. (2022). Leukemia. StatPearls Publishing, 2022. https://www.ncbi.nlm.nih.gov/books/NBK560490/.

[15] Khan, S., Rahmani, H., Shah, S.A. A., Bennamoun, M. (2018). A guide to convolutional neural networks for computer vision. Synthesis Lectures on Computer Vision, 1-207. https://link.springer.com/book/10.1007/978-3-031-01821-3.

[16] Simonyan, K., Zisserman, A. (2015). Very deep convolutional networks for large-scale image recognition.

International Conference on Learning Representations (ICLR), San Diego, CA, USA.

[17] He, K.M., Zhang, X.Y., Ren, S.Q., Sun, J. (2016). Deep residual learning for image recognition. IEEE Conference on Computer Vision and Pattern Recognition (CVPR), Las Vegas, NV, USA, 2016, pp. 770-778. https://doi.org/10.1109/CVPR.2016.90

[18] Choi, D., Shallue, C.J., Nado, Z., Lee, J., Maddison, C.J., Dahl, G.E. (2019). On empirical comparisons of optimizers for deep learning. https://arxiv.org/pdf/1910.05446.pdf, accessed on Oct. 20, 2022.

[19] Ruder, S. (2019). An overview of gradient descent optimization. https://arxiv.org/pdf/1609.04747.pdf, accessed on Oct. 21, 2022.

[20] Kingma, D.P., Ba, J.L. (2015). ADAM: A Method for stochastic optimization. 3rd International Conference on Learning Representations (ICLR), San Diego, CA, USA, 2015. https://doi.org/10.48550/arXiv.1412.6980

[21] Dalianis, H. (2018). Evaluation Metrics and Evaluation. Clinical Text Mining, 1, Springer, Cham, 2018, 45-53. https://doi.org/10.1007/978-3-319-78503-5_6

[22] Chen, Y.M., Chou, F.I., Ho, W.H., Tsai, J.T. (2021). Classifying microscopic images as acute lymphoblastic leukemia by resnet ensemble model and taguchi method. BMC Bioinformatics, 22(Suppl 5): 615. https://doi.org/10.1186/s12859-022-04558-5

[23] Shah, S., Nawaz, W., Jalil, B., Khan, H.A. (2019). Classification of Normal and Leukemic Blast Cells in B ALL Cancer Using a Combination of Convolutional and Recurrent Neural Networks. Springer Nature Singapore Pte Ltd, 2019. https://doi.org/10.1007/978-981-15-0798-4_3

[24] Vogado, L.H.S., Veras, R.M.S., Aires, K.R.T. (2021). LeukNet - A Model of Convolutional Neural Network for the Diagnosis of Leukemia, pp. 119-125. https://doi.org/10.5753/sibgrapi.est.2020.12993

[25] Shah, S., Nawaz, W., Jalil, B., Khan, H.A. (2019). Classification of Normal and Leukemic Blast Cells in B-ALL Cancer Using a Combination of Convolutional and Recurrent Neural Networks. In: Gupta, A., Gupta, R. (eds) ISBI 2019 C-NMC Challenge: Classification in Cancer Cell Imaging. Lecture Notes in Bioengineering. Springer, Singapore. https://doi.org/10.1007/978-981-15-0798-4_3